A supercritical CO_2 assisted electrohydrodynamic process used to produce microparticles and microfibers of a model polymer

Lucia Baldino, Stefano Cardea, Ernesto Reverchon*

Department of Industrial Engineering, University of Salerno, Via Giovanni Paolo II, 132, 84084, Fisciano (SA), Italy

Corresponding author information:

ereverchon@unisa.it; +39089964116; www.supercriticalfluidgroup.unisa.it

Abstract

An evolution of traditional electrospray and electrospinning is proposed in this work, adding SC-CO_2 in the liquid polymeric solution. This new process arrangement allows to overcome some intrinsic limitations of the traditional processes, namely surface tension and viscosity control. The influence of various process parameters was studied. The increase of electric potential difference did not significantly modify the particle size distributions and the fiber size distributions; but, the distributions became sharper as the electric potential difference increased. At low PVP percentages in the solution, electrospray was favored, forming small particles, due to low solution viscosity. The viscosity of the solution increased with PVP concentration: therefore, first large and very large particles were formed; then, the process was no more able to produce jet break-up, microfibers were obtained and the process was converted to electrospinning, producing microfibers with diameters down to about 1.4 μm. Using lower molecular weight PVP, smaller particles (down to 0.35 μm) were produced and the particles/fibers transition occurred at larger polymer percentages. Pressure and PVP percentage played opposite roles in generating the different morphologies; therefore, electrospray and electrospinning assisted by SC-CO_2 are like two faces of the same medal: they could be performed using the same apparatus, properly setting the process conditions and polymer concentration.

Keywords: electrospray; electrospinning; supercritical CO_2; microparticles; microfibers.

1. Introduction

Several industrial fields can take advantage of the production of micro and nanoparticles and micro and nanofibers in a controlled way. Therefore, the production of these materials has been attempted using several techniques. Micro- and nano-particles production has been performed using traditional techniques like jet-milling, spay drying, microgrinding, micro- and nano-emulsions, etc. [1-5]. Microfibers, with a diameter of several microns, are commonly produced by melt extrusion and cold-drawing [6,7]. Some advanced techniques have been also proposed to reach these targets. For example, supercritical CO_2 (SC-CO_2) based processes like supercritical antisolvent (SAS) [8], supercritical assisted atomization (SAA) [9], rapid expansion of a supercritical solution (RESS) [10] and its modifications [11], and supercritical emulsion extraction (SEE) [12], only to cite the most famous SC-CO_2 based techniques to obtain micro and nanoparticles.

Two electrohydrodynamic (EHD) based techniques are also largely discussed in the literature to produce microparticles and microfibers. They are characterized by the application of an electric potential difference between a nozzle and a collector to obtain the Taylor's cone formation or the jet beak-up, producing fibers or particles, respectively. The first process is named electrospinning (ESP) [13-15]; the second one is commonly called electrospraying (ESPR) [16-18].

In particular, electrospraying is based on the atomization of a solution through a nozzle, due to a potential difference between the nozzle tip and a ground electrode. If the applied voltage overcomes the cohesive forces of the liquid solution (mainly surface tension and viscosity), droplets are formed and it is possible to produce micro- or nano-particles [16].

If liquid jet break-up is not obtained, fibers instead of droplets are obtained, and electrospinning is performed [14]. The main parameters that can influence the transition between droplets and the formation of fibers in EHD techniques are solution viscosity and surface tension.

However, these techniques suffer of some limitations. Electrospray requires very small solution flow rates, frequently of the order of microliters/hour [16]. As a consequence, it can produce very reduced quantities of particles, that could be generally used as a "proof of concept" more than for a possible practical application. Electrospinning, in all traditional configurations, has to face intrinsic limitations related to surface tension and viscosity of the spinned solutions: high surface tension and high viscosity mixtures cannot be successfully processed [19,20]. Moreover, in both processes, possible toxic organic solvent residues can pollute the final products, representing a relevant drawback especially for pharmaceutical and biomedical applications.

Until now, only some attempts at the introduction of SC-CO_2 in electrohydrodynamic processes have been performed. Levit and Tepper [21] demonstrated that the presence of SC-CO_2 in the precipitation vessel, reduced polymer viscosity and it was sufficient to allow fibers to be electrostatically pulled from a bulk polymer sample. Operating in this manner, polymer fibers of a high molecular weight polydimethylsiloxane (PDMS) and poly(d,l-lactic acid) (PLA) were produced at 40 °C and 140 bar, using only electrostatic forces, without the use of a liquid solvent. Lee et al. [22] added SC-CO_2 as non-solvent in the precipitation vessel to allow the rapid elimination of the organic solvent from polyvynilpyrrolidone (PVP) fibers during electrospinning. Moreover, SC-CO_2 diffusion inside the fibers promoted the generation of a nanoporous morphology. Liu et al. [23] proposed again electrospinning in presence of SC-CO_2, as anti-solvent, to produce micron to submicron polymeric fibers of PVP and poly(vinylidenefluoride) (PVDF), with open-cell or hollow core morphology. Li et al. [24] used a similar electrospinning process to produce porous or hollow nanofibers of PVP. Okamoto and Wahyudiono [25] performed electrospinning in high-pressure carbon dioxide to reduce the viscosity of a PVP:PLLA solution (80:20) in dichloromethane. Fibers without beads formation were produced, with diameters ranging between 0.60-0.79 μm. Wahyudiono et al. [26] produced PVP hollow fibers by electrospinning of a solution in pressurized carbon dioxide. Depending on operative pressure, different PVP morphologies were obtained: solid fiber at 30 bar, hollow core fibers at 50 bar and balloon-like structures at 80 bar. All these techniques are not particularly encouraging since SC-CO_2 was added in a high pressure vessel. The process arrangement was very complex with respect to the traditional one since fibers formation required a close, high pressure precipitator that poses several limitations to process flexibility and products collection. Li et al. [27] used compressed nitrogen instead of CO_2, to produce PVP fibers by electrospinning. As in the previous cases, the role of nitrogen was as non-solvent. However, these authors concluded that nitrogen was not a good choice for producing hollow or porous PVP nanofibers.

To overcome the limitations observed in the previous SC-CO_2 based processes, it should be possible to develop an electrospraying and electrospinning processes assisted by SC-CO_2 (SA-EHDP), in which supercritical CO_2 is added to the polymeric liquid solution before precipitation, largely reducing its viscosity and surface tension (i.e., cohesive forces); in this case, an expanded liquid (GLX) is formed, in which dissolved SC-CO_2 influences cohesive forces and their modification can be modulated selecting the molar fraction of dissolved CO_2 [28-30]. Moreover, a high pressure vessel precipitator is no more required and materials collection can be performed in the usual way. The concept of GLX has been previously applied in processes like SAA and SAS, mentioned in this Introduction.

A recent paper [31] reports the feasibility of a new technique, called supercritical assisted electrospraying (SA-ESPR), in which the addition of SC-CO_2 to a starting polymeric liquid solution, produced controlled size micro- or nano-particles. In particular, for the first time, SC-CO_2 was added to the polymeric liquid solution, before the spraying process, forming an expanded liquid. Operating in this way, surface tension and viscosity of the polymeric solution were effectively reduced, allowing the production of micrometric or nanometric particles of controlled size and distribution at a production rate up to hundred times than the traditional electrospray process. However, the control of process pressure was problematic, only particles were produced in a limited range of concentrations.

The scope of this work is to develop an evolution of this technology, devoted not only to the production of micro- and nano-particles; but, also to the production of micro- and nano-fibers of PVP, through the adoption of a more advanced configuration of the process. A systematic analysis of process parameters like polymer molecular weight, polymer concentration in the solution, pressure and voltage will be performed, trying to show that it is not only possible to overcame the previously discussed limitations of the electrohydrodynamic processes, but, electrospray and electrospinning assisted by SC-CO_2 are like the two faces of the same medal: they could be performed using the same apparatus, properly setting the process conditions and polymer concentration.

2. Materials, apparatus and methods

Polyvinylpyrrolidone (PVP, M_w 1,300,000 and 10,000) and ethanol (purity >99.9%) were bought from Sigma Aldrich. CO_2 (purity 99.9%) was supplied by Morlando Group s.r.l. (Sant'Antimo, NA, Italy).

PVP powder was dissolved in ethanol at different concentrations by weight (ranging from 1 to 15% w/w), at room temperature and using a magnetic stirrer at 100 rpm.

The SA-EHDP apparatus mainly consisted of a stainless-steel high-pressure vessel with an internal volume of 72.3 mL (feeding vessel), in which a PVP-ethanol solution was loaded. The vessel was closed and CO_2 was pumped from the bottom using a high-pressure pump (Gilson, mod. 305, Middleton, WI, USA) up to the desired pressure. When the desired process pressure was reached, the system was left 10 min for equilibration, to favor the mixing between SC-CO_2 and the liquid polymeric solution in order to obtain an expanded liquid [28-31]. To allow a constant pressure operation, after this time, nitrogen was introduced from the top of the vessel at the same pressure selected for the process. Operating in this way, N_2 counter balanced pressure reduction during the progressive discharge of the vessel, allowing process development at constant pressure. A Teflon disk located on the top of the liquid solution avoided the contact and thus the diffusion of N_2 in the liquid solution during processing. Operating in this way and opening an ON/OFF valve (Swagelok ON/OFF, Nordival s.r.l., Rovato (BS), Italy), the polymeric solution was delivered from the vessel to a 100 μm internal diameter injector, responsible of the atomization/spinning process. The area near the injection system was heated using cable heaters (Watlow, 240 V, 275 W) to counter balance the freezing Joule-Thomson effect, related to a fast CO_2 depressurization. Temperature was measured by thermocouples and regulated using PID controllers (mod. 305, Watlow, Corsico (MI), Italy); whereas, pressure in the feeding vessel was measured by a test gauge (mod. MP1, OMET, Lecco, Italy). The voltage generator was a FUG Elektronik (mod. HCP 35-3500, Schechen, Germany). The collector was composed by two adjacent stainless-steel blocks, covered by a thin aluminum foil. An experiment ended when the whole content of the feeding vessel was discharged; each experiment was repeated twice.

To measure the quantity of CO_2 dissolved in the PVP-ethanol solution, in a separate series of experiments, the vessel was loaded with 50 mL of solution and pressurized up to the required pressure (80, 100, 120, 140 and 160 bar). Then, the vessel was allowed to slowly depressurize through a needle valve (mod. SS-20VS4 Swagelok, Nordival s.r.l., Rovato (BS), Italy) connected to a volumetric gas counter (G2.5, Sacofgas, Milan, Italy). Operating in this way, the volume of CO_2 dissolved in the solution was measured at atmospheric pressure and room temperature. The comparison with the number of moles of ethanol loaded in the vessel, allowed the calculation of the mole fraction of CO_2 dissolved in the polymeric solution at the different pressures explored.

PVP processed samples were sputter coated with gold (Agar Auto Sputter Coater mod. 108 A, Stansted, UK) at 30 mA for 80 s and analyzed using a field emission scanning electron microscope (FE-SEM, mod. LEO 1525, Carl Zeiss SMT AG, Oberkochen, Germany) to study their morphology.

Sigma Scan Pro 5.0 (Jandel scientific, San Rafael, QC, Canada) and Origin 9.1 (Microcal, Northampton, MA, USA) were used to determine the average diameter of the particles or of the fibers and to calculate the size distributions. Approximately 300 particle and fiber diameters were measured for each calculation.

Differential scanning calorimetry (DSC 30 Mettler, Toledo, Spain) was carried out to analyze and identify any changes in the thermogram of processed polymer, compared with the one of PVP starting powder. Calorimetric analysis was performed in the temperature range between 25 °C and 150 °C, with a heating rate of 10 °C/min; the inert gas was nitrogen, at a flow rate of 50 L/min.

3. Results and discussion

At the selected operating conditions (35 °C, pressure from 80 to 160 bar), a monophasic gas expanded liquid (GXL) is formed when SC-CO_2 is added to the liquid mixture loaded in the feeding vessel. Indeed, looking at CO_2-ethnaol high pressure phase behavior, as reported for example in the literature by Joung et al. [32] and Tanaka et al. [33], working at 35 °C and pressures larger or equal to 80 bar, a monophase GLX is always formed, whichever x_{CO2} is selected that occupies the whole vessel internal volume.

Some preliminary measurements were performed to calculate the quantity of CO_2 dissolved in the liquid solvent alone (ethanol) and in the polymeric solution. 50 mL of ethanol or of the ethanolic solution were generally loaded; temperature was set at 35 °C. Using the experimental procedure described in Materials, Apparatus and Methods, CO_2 molar fraction was measured at the various pressures tested in this work (80, 100, 120, 140 and 160 bar). The experimental procedure adopted produced a quasi constant CO_2 number of moles dissolved in the liquid phase. Since ethanol volume was 50 mL, the corresponding CO_2 molar function was consequently between 0.61 and 0.63. This result is not surprising since compressibility of GLXs is very reduced; it is more similar to the one of liquids and tends to decrease with pressure [28,30], becoming almost constant at pressures above about 120 bar [28,30]. Similar experiments were performed also adding various polymer (PVP) percentages to ethanol; also in these cases, 50 mL of ethanolic solution were loaded. A reduction of CO_2 quantity dissolved in the solution was observed that, however, was practically constant with PVP weight percentages between 1 and 10% and varying the operating pressure. CO_2 molar fraction was calculated taking into account only the presence of ethanol; i.e., performing a solute free basis calculation. Calculated CO_2 molar fraction on solute free basis ranged between about 0.54 and 0.57. An experiment was also performed reducing the quantity of ethanolic solution loaded in the feeding vessel at 20 mL. In this case, a larger quantity of CO_2 dissolved into the solution; i.e., reaching a molar fraction of about 0.81. This last result is readily explainable taking into account that in this experiment a larger expansion was allowed to the GLX before the further pressurization at constant volume. All this information is very relevant looking at a calculation of the influence of CO_2 molar fraction on the performance of the process and to transfer the results to other apparatuses: i.e., reproducibility and scale up of the process.

At this point of the study, systematic experiments were performed. All experimental series were carried out maintaining constant these parameters: diameter of the injector at 100 μm, injector-collector distance at 25 cm, process temperature at 35 °C and 50 mL ethanolic solution. Process parameters analyzed in this study are: voltage, PVP concentration in the solution, PVP molecular weight and operative pressure.

Effect of voltage

This parameter is the most characteristic of electrospraying and electrospinning [20]. As explained in the Introduction, the forces exerted by the different voltages (also called electric potential difference, ΔV) are responsible of the atomization or of the spinning of the polymeric solution.

Experiments were performed at 120 bar, PVP molecular weight of 1300000 and ΔV= 10, 20, 30 kV and, then, modifying polymer concentration. A first fundamental experiment was performed setting the electric potential difference to zero. Indeed, also pressurization of the liquid solution and its exit from a nozzle, could be, in principle, capable to activate an atomization process. During this experiment, only dipping of the liquid solution was observed, at the lower polymer concentrations tested. Then, a series of experiment was performed applying different voltages and using PVP concentrations from 1 to 15% w/w in ethanol.

Microparticles were produced at 10 kV. Figure 1 reports an example of these particles, obtained using a 3% w/w PVP ethanolic solution. Particles were spherical and not coalescing.

Figure 2 reports diameters distribution obtained for these particles, at 10, 20 and 30 kV. They were characterized by a mean diameter located at about 1 µm. The increase of electric potential difference did not significantly modify the mean of these distributions; but, the distribution was sharper as the electric potential difference increased.

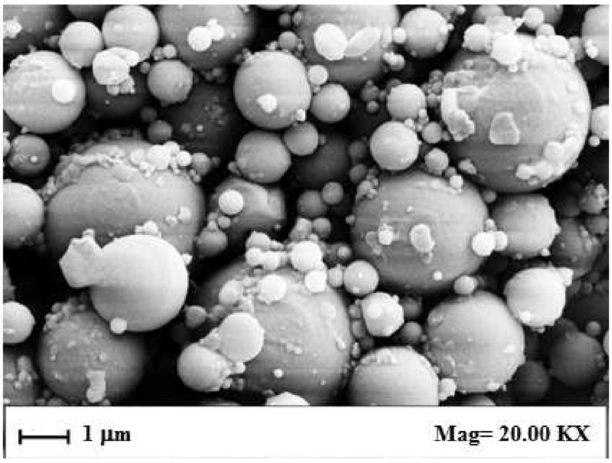

Figure 1. PVP particles produced at 10 kV, starting from a 3% w/w PVP ethanolic solution.

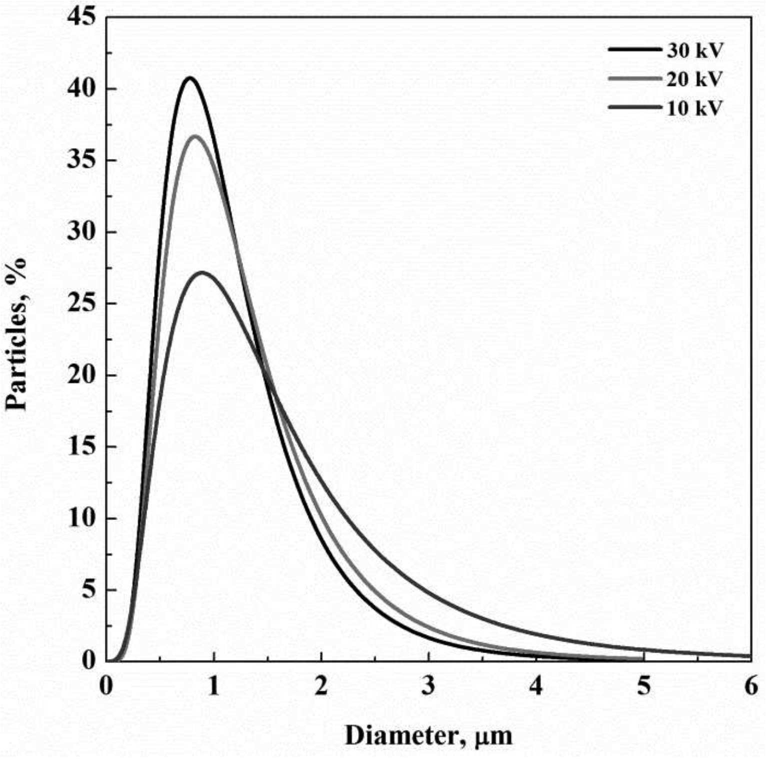

Figure 2. PVP 3% w/w particles mean diameter variation depending on applied voltage.

A similar effect was observed also in the experiments performed at 1% w/w PVP, as shown in Figure 3. Particles were sub-micrometric with a mean diameter located at about 0.5 μm.

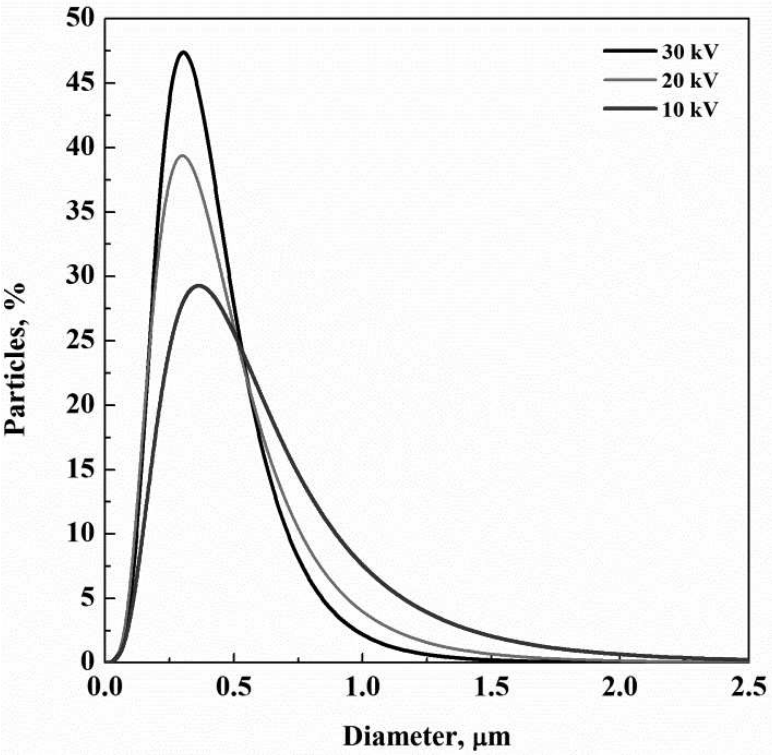

Figure 3. PVP 1% w/w particles mean diameter variation depending on applied voltage.

These results can be explained considering that an increase of voltage improved the regularity of the atomization process, conferring more uniformity to the droplets produced and, consequently, to microparticles obtained: the final result was the sharpening of PSD.

Processing ethanolic solution containing 5% w/w PVP, microparticles and microfibers were observed in the sample obtained, operating at 10 kV (Figure 4a); whereas, at 20 and 30 kV, only microparticles were again produced (Figure 4b-c). When larger PVP percentages (10% and 15% w/w) were processed using different electric potentials, microfibers only were observed in the precipitates starting from a voltage of 10 kV, as shown in the SEM image reported in Figure 4d. Operating at 15% w/w PVP, microfibers were produced at all the electric potential differences tested; a further example of this morphology is reported in Figure 4e. The regularity of microfibers also decreased increasing electrical potential difference, as it can be observed comparing Figures 4d and 4e.

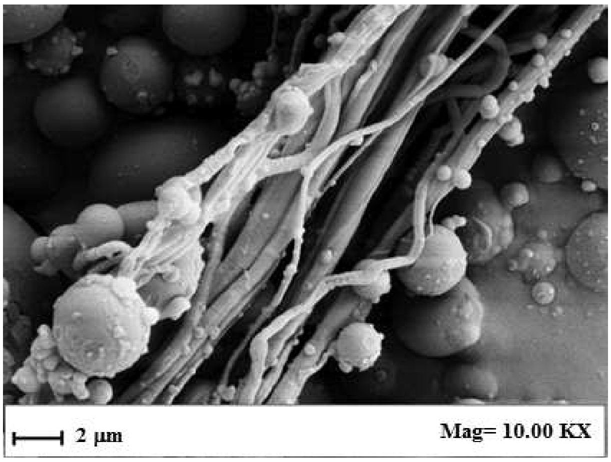

(a)

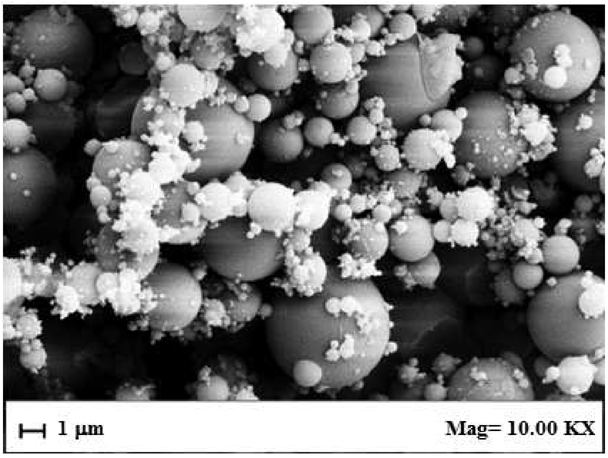

(b)

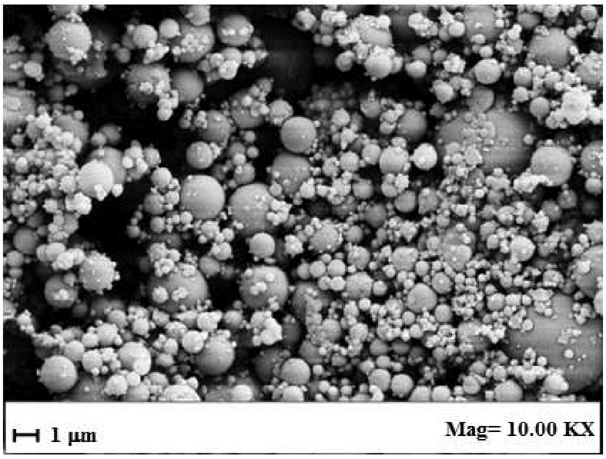

(c)

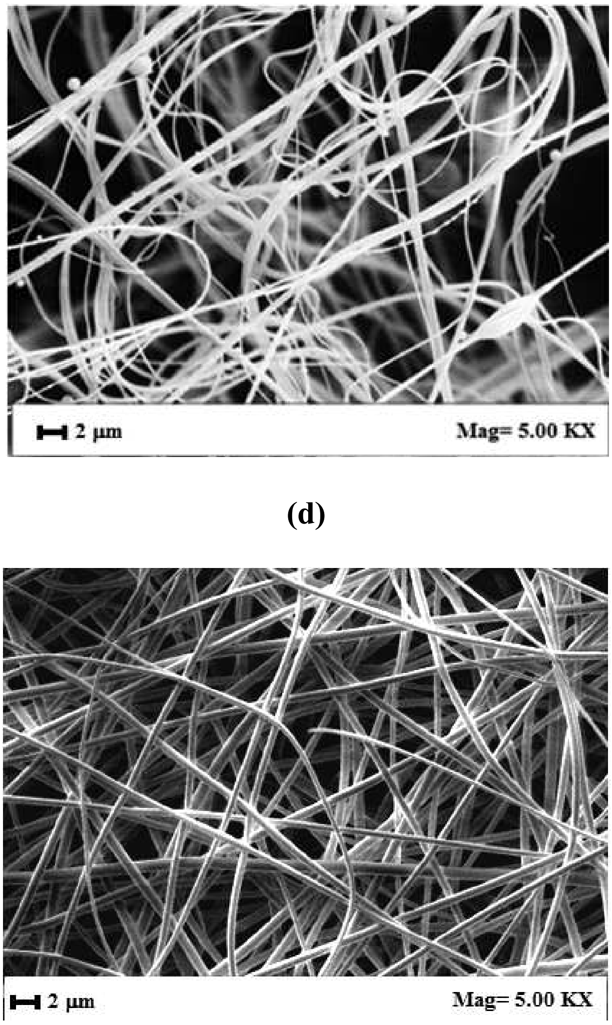

(d)

(e)

Figure 4. SEM pictures of PVP products obtained starting from: 5% w/w PVP concentration and working at (a) 10 kV, (b) 20 kV, (c) 30 kV; (d) 10% w/w PVP concentration, working at 10 kV; (e) 15% w/w PVP concentration, working at 30 kV.

All these results have been condensed in Figure 5, where the morphologies observed are reported at the different PVP percentages tested, against the different voltages applied. This diagram indicates two distinct regions in which only microparticles or only microfibers were formed and a transition from microparticles to microfibers. The explanation of these results is relatively simple: increasing the percentage of PVP, solution viscosity increased, that is a powerful cohesive force. Increasing electrical potential difference, disgregative forces were increased, instead. This explanation can be clearer looking, in more details, at the atomization process: during atomization, at the exit of the injector, first a continuous liquid jet is observed, then, jet break-up is produced and droplets are formed. In the case of fibers formation, when cohesive forces overcome dissipative ones, jet break-up was no more observed but, due to the presence of a ΔV, the process developed a Taylor's cone [17,18] with the formation of microfibers.

At the best of the authors knowledge, this is the first time that using the same apparatus and process conditions, it has been possible to produce microparticles or microfibers, only selecting polymer concentration against the electric potential difference.

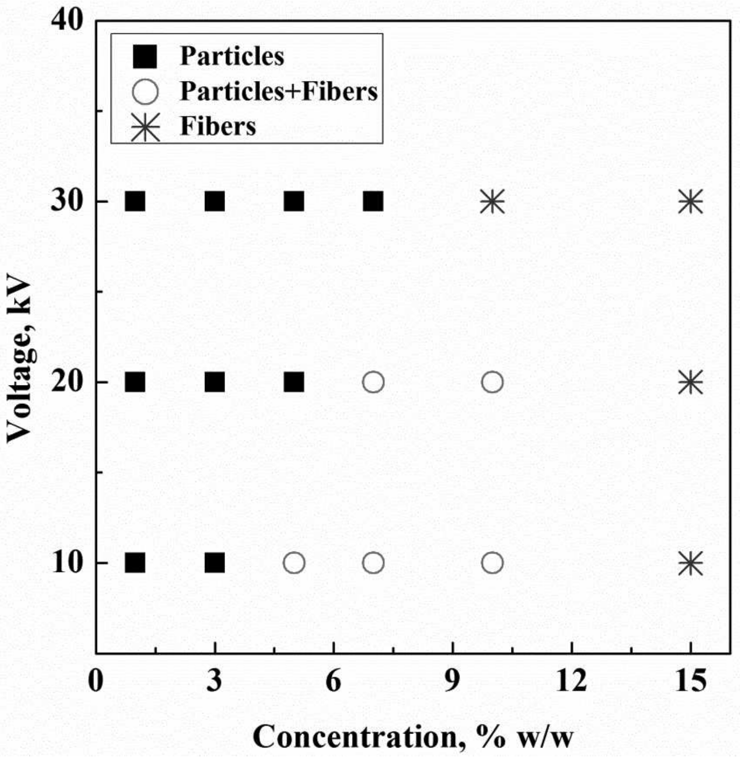

Figure 5. Graphical representation of particles and fibers, depending on voltage and PVP concentration.

Effect of PVP concentration

Set the pressure at 120 bar and the voltage at 30 kV, the effect of PVP concentration by weight in the ethanolic solution was analyzed at different PVP molecular weights. All these results are synthetically reported in Table 1.

PVP concentration	**Mean diameter ± standard deviation**	
	M_w=10000	**M_w=1300000**
1% w/w	0.340 ± 0.195 µm	0.434 ± 0.199 µm
3% w/w	0.585 ± 0.321 µm	1.320 ± 0.772 µm
5% w/w	1.005 ± 0.648 µm	1.703 ± 0.780 µm
7% w/w	1.740 ± 0.873 µm	5.813 ± 3.431 µm
10% w/w	2.234 ± 0.987 µm	1.641 ± 0.890 µm*
15% w/w	1.387 ± 0.499 µm*	1.741 ± 0.895 µm*

*Microfibers.

Table 1. Particles and fibers mean diameter at different PVP molecular weight and concentration, tested in this work.

For PVP1300000, microparticles were observed operating at PVP percentages by weight from 1 to 7% in ethanol; at higher polymer concentration, fibers were produced. The corresponding particle size distributions (PSD$_s$) are reported in Figure 6, in which an increase of the mean diameter from 0.43 to 5.81 µm and a pronounced enlargement of the size distribution is evident.

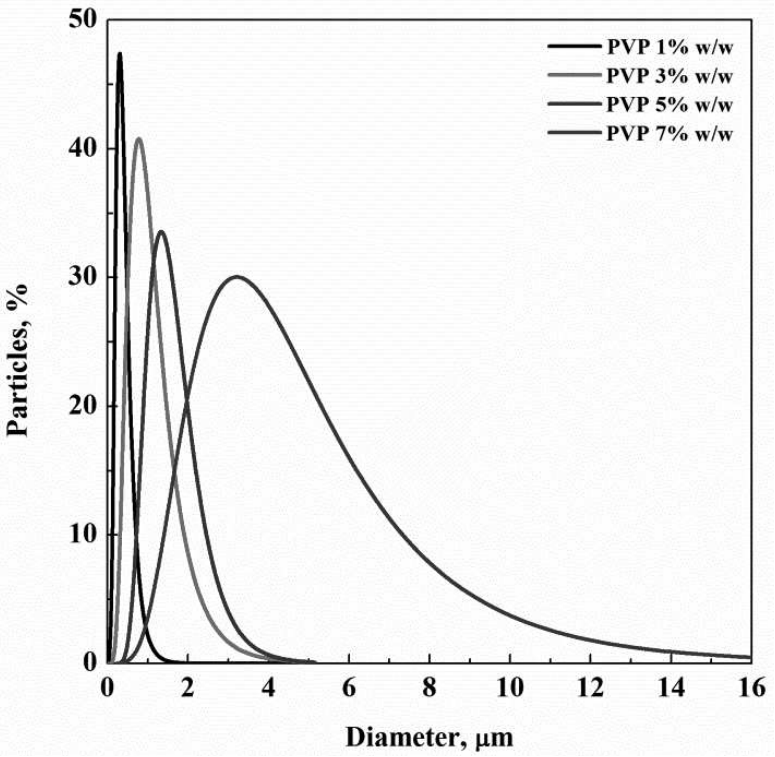

Figure 6. PSD$_s$ of PVP particles, produced at 120 bar and 30 kV and at different PVP concentrations.

It is interesting to note that the increase of the mean particles diameter was largely non linear with the polymer concentration, as shown in Figure 7. Indeed, until concentrations of PVP up to 5% w/w were used, only a relatively small influence of concentration on particle size was observed; then, its influence became very pronounced. This result should depend on the viscosity of the starting solution: large particles (diameter of about 6 µm) were produced only in the proximity of the transition between particles and fibers. The experiments performed at 10% w/w and at higher PVP percentages produced fibers, as previously indicated in Figure 5. Fibers diameter also increased with PVP weight percentage (see Table 1). Of course, the increase of solution viscosity explains also this result.

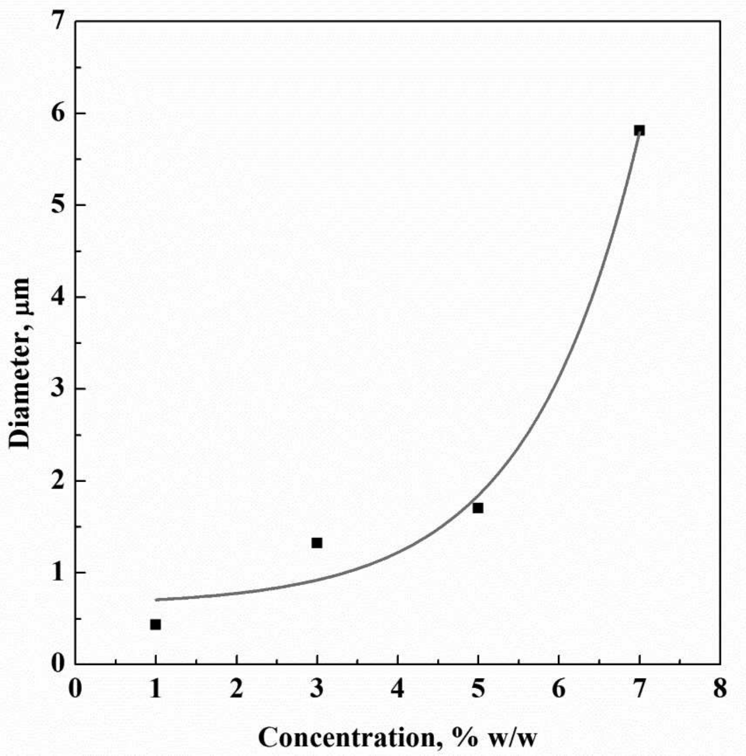

Figure 7. Particles mean diameter variation depending on PVP weight concentration.

Commenting this data set, it is interesting to note that the explanation previously given about the balance between cohesive and disruptive forces, justifies also these results: at low PVP percentages, the electrohydrodynamic based process was favored in forming smaller particles, due to low solution viscosity. When solution viscosity increased, first large and very large particles were formed with an enlargement of the PSD; then, the process was no more able to generate jet break-up and microfibers were produced, whose diameters were also correlated with solution viscosity. Examples of particles and fibers observed in this part of the study are reported in Figure 8.

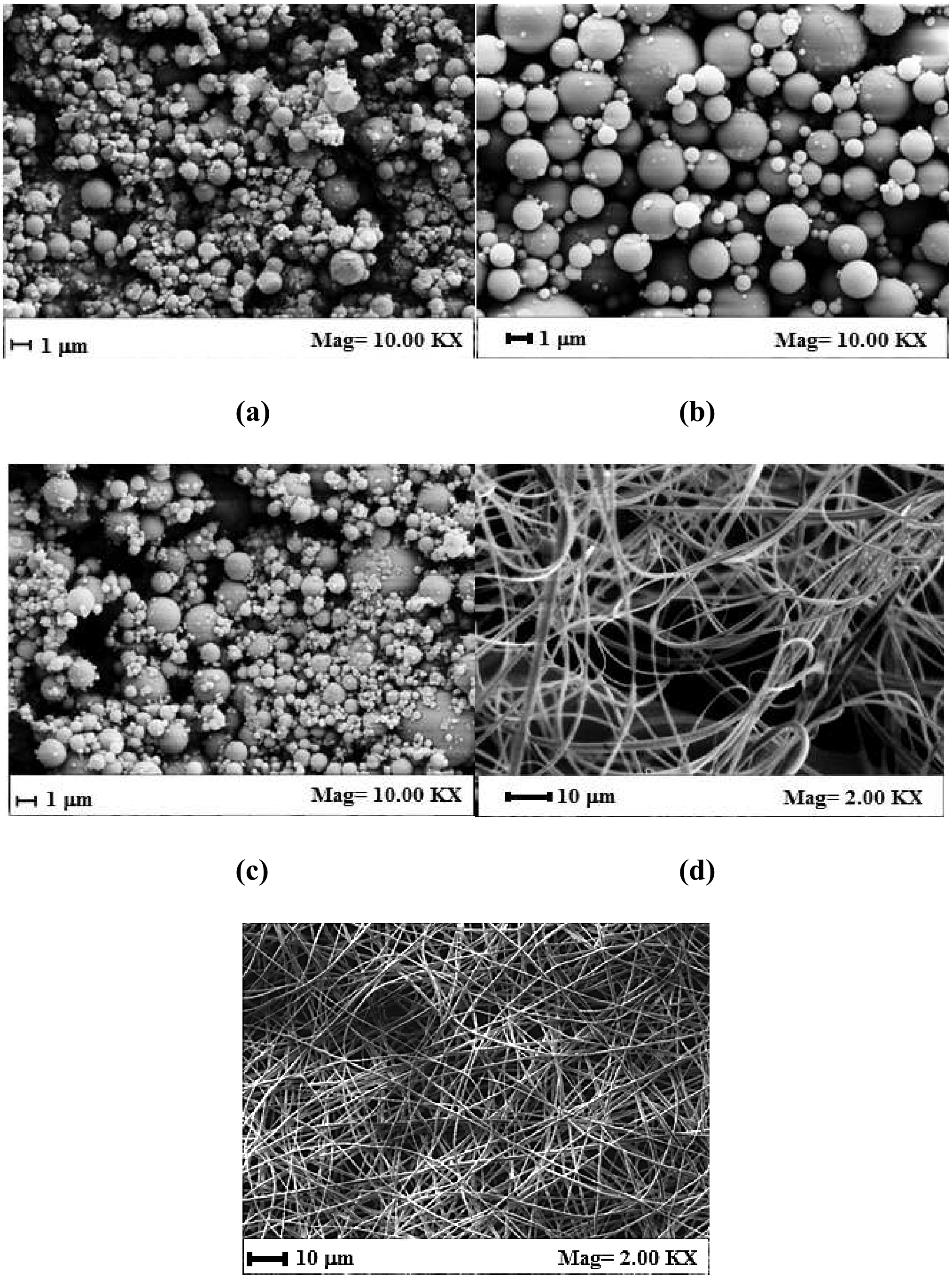

(a) **(b)**

(c) **(d)**

(e)

Figure 8. SEM images of PVP samples obtained at: (a) 1% w/w, (b) 3% w/w, (c) 5% w/w, (d) 10% w/w, (e) 15% w/w. P= 120 bar, ΔV= 30 kV.

Effect of PVP molecular weight

Another parameter that can influence morphology and diameter of the materials produced using SA-EHDP is the molecular weight of the polymer selected. Indeed, molecular weight influences viscosity of the solution formed. In all previous experiments, a PVP molecular weight of 1300000 was used. In this series of experiments, PVP with a low molecular weight (i.e., 10000) was tested. Again, a pressure of 120 bar was adopted and voltage was set at 30 kV. The experiments were performed at PVP concentrations between 1% and 15% w/w in ethanol and are, thus, comparable with those performed at the same conditions, but using the high molecular weight PVP.

The results are summarized in Table 1, columns first and second. Also in this case, microparticles were observed at lower PVP percentages; but, their particle size and the amplitude of their PSD were smaller with respect to those observed in PVP1300000 experiments. For example, operating with a PVP percentage of 1% w/w, using PVP10000, the mean diameter of the particles was 0.34 μm, instead of 0.43 μm, measured for PVP1300000. Operating at a PVP percentage of 7% w/w, PVP10000 particles showed a mean diameter of 1.74 ± 0.87 μm; whereas, PVP1300000 particles showed a mean diameter of 5.81 ± 3.43 μm. Not only in the second case the particles were more than three times larger, but also the standard deviation was more than three times larger (Table 1). Another relevant difference is that PVP10000 showed the change of morphology from particles to fibers, at a PVP percentage around 15% w/w, instead that around 10% w/w.

Summarizing these results, a lower molecular weight PVP, due to the lower intrinsic viscosity connected to the relative motion of the polymer chains and to the lower effect of polymer entanglements, produced smaller particles and the particles/fibers transition occurred at higher polymer percentages.

Effect of pressure

This is in principle one of the most promising parameter of SA-EHDP process; it is new with respect to the traditional EHD processes and operates as an additional disgregative force on the liquid solution at the exit of the injector.

Selecting PVP molecular weight at 1300000 and voltage at 30 kV, pressures between 80 and 160 bar were explored, using PVP percentages between 1% and 15% w/w. The results obtained operating at PVP 1% w/w and pressures between 80 and 160 bar are shown in Figure 9. A continuous reduction of particles size was observed, accompanied by a sharpening of the PSD. Moreover, PSDs in Figure 9 give a clear demonstration of the trends observed: operating at 160 bar, PVP sub-microparticles with a mean diameter of 0.26 µm were measured. Similar trends were also observed in the series of experiments performed at PVP percentages of 3% and 5% w/w.

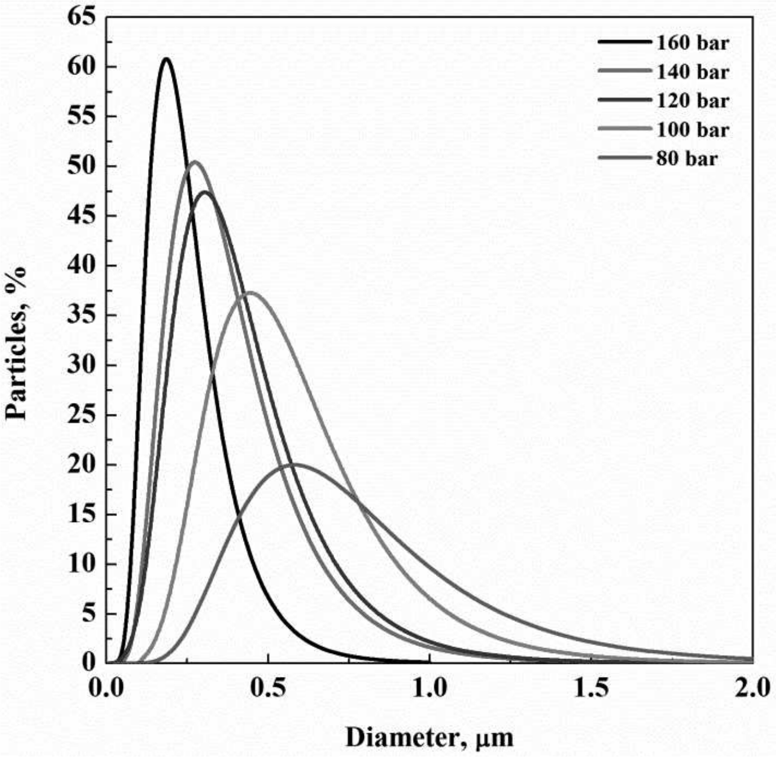

Figure 9. PSD$_s$ of 1% w/w PVP particles, produced at 30 kV and different pressures.

However, as expected, increasing PVP percentage in the starting solution, larger particles were obtained. For example, particles produced from a PVP solution at 5% w/w showed a mean diameter of 0.93 µm; using PVP solution at 7% w/w, the transition from microparticles to microfibers was observed, reducing the process pressure at 100 bar. The transition between the two morphologies moved to 120 bar at 10% w/w PVP and completely disappeared at 15% w/w PVP, in the range of pressures explored. It is interesting also to monitor the microfibers diameter that at 15% w/w PVP decreased from 4.15 µm to 0.77 µm, varying the pressure from 80 to 160 bar. These last results are summarized in Figure 10, where size distribution of fibers diameter (FSD$_s$) are shown.

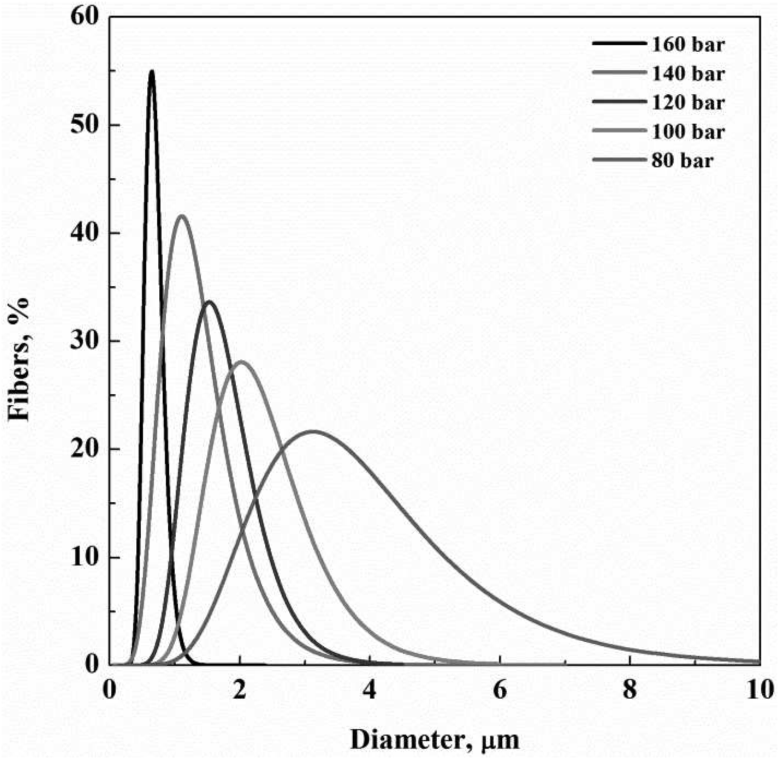

Figure 10. FSD$_s$ of 15% w/w PVP fibers, produced at 30 kV and different pressures.

Summarizing the results obtained in this part of the work, it is possible to propose the diagram in Figure 11 that reports the morphologies observed varying pressure against PVP percentage in the starting solution. Similarly to the diagram previously reported at different voltages, this diagram gives a map with the location of the two morphologies in the plane concentration-pressure and allows to follow the transition observed. As expected, pressure and PVP percentage play opposite roles in generating the different morphologies, being pressure a disruptive force and PVP percentage a cohesive force due to the increase of viscosity of the starting solution. The different balance of these two forces determines the observable morphology.

It is interesting to note, also, that in this series of experiments, the change between the two morphologies was not accompanied by an evident transition region.

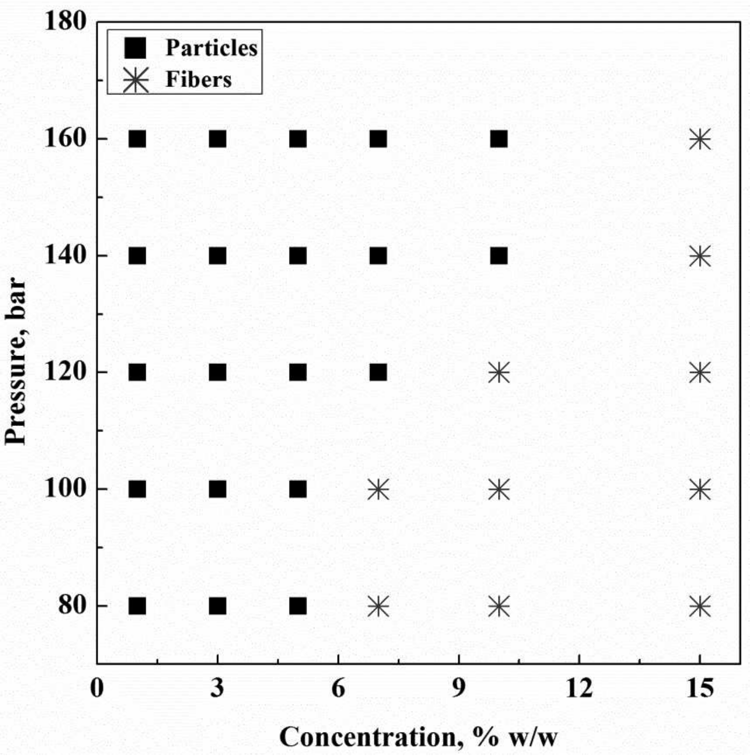

Figure 11. Graphical representation of particles and fibers, depending on pressure and PVP concentration.

Other characterizations

Figure 12 reports DSC analysis of unprocessed PVP and of a PVP sample after processing. In the first case, the thermogram is characterized by a large peak from about 60 °C to about 110 °C (first curve from the bottom), related to water evaporation from the polymer hydrophilic groups; whereas, the thermogram related to the PVP sample after processing (second curve from the bottom), shows and endothermic peak in the temperature range of 40-80 °C. These results are consistent with the literature [34] and demonstrate that, during this process, water molecules are also massively eliminated from the polymer.

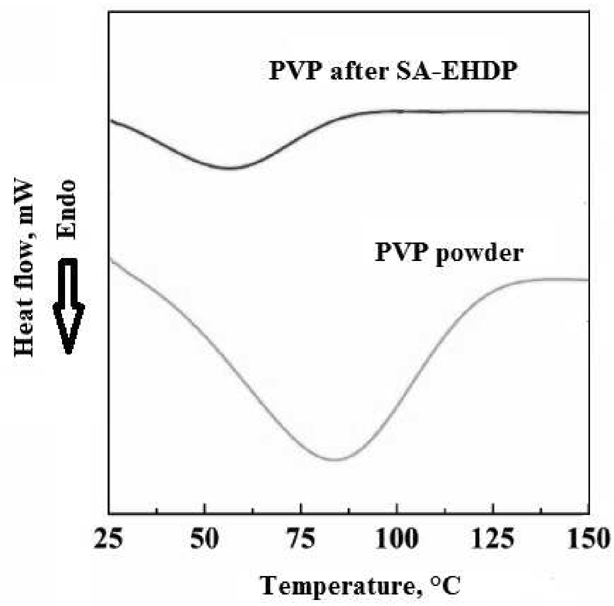

Figure 12. DSC analyses on unprocessed PVP powder and PVP sample after processing.

4. Conclusions and perspectives

SA-EHDP process, in the configuration presented in this work, maintained the promises of being a stable and flexible process. It was possible to produce PVP sub-microparticles or fibers at high production rates, with a good control over their diameter and distribution. One further interesting feature was the possibility to switch from one morphology to the other, without changing the process arrangement. The results obtained have been explained in terms of the balance between cohesive and disruptive forces in the atomization process.

The contribution of CO_2 dissolved in the starting liquid polymeric solution is relevant, since its presence in the formed GLX, reduces the surface tension of the liquid to be processed and its viscosity. It also introduces a large flexibility in the process with respect to the classical electrospray and electrospinning.

In the next future, other polymers will be tested, composite (polymer+drug) microparticles or fibers will also be produced to test other applications of this new process arrangement.

References

[1] G. Nykamp. U. Carstensen, B.W. Müller, Jet milling—a new technique for microparticle preparation, Int. J. Pharm. 242 (2002) 79-86.

[2] F. Sansone, T. Mencherini, P. Picerno, M. d'Amore, R.P. Aquino, M.R. Lauro, Maltodextrin/pectin microparticles by spray drying as carrier for nutraceutical extracts, J. Food Eng. 105 (2011) 468-476.

[3] E. Brinksmeier, O. Riemer, S. Kirchberg, C. Brandao, Injection molded spherical grinding tools: manufacture and application of a novel tool concept for micro grinding, Prod. Eng. 7 (2013) 383-389.

[4] A. Gupta, H. Burak Eral, T. Alan Hatton, P.S. Doyle, Nanoemulsions: formation, properties and applications, Soft Matter 12 (2016) 2826-2841.

[5] S.S. Bansode, S.K. Banarjee, D.D. Gaikwad, S.L. Jadhav, R.M. Thorat, Microencapsulation: A review, Int. J. Pharm. Sci. Rev. Res. 1 (2010) 38-43.

[6] X.-B. Xu, Z.-M. Li, R.-Z. Yu, A. Lu, M.-B. Yang, R. Huang, Formation of in situ CB/PET Microfibers in CB/PET/PE Composites by Slit Die Extrusion and Hot Stretching, Macromol. Mater. Eng. 25 (2004) 568-575.

[7] V. Jašo, M.V. Rodić, Z.S. Petrović, Biocompatible fibers from thermoplastic polyurethane reinforced with polylactic acid microfibers, Eur. Polym. J. 63 (2015) 20-28.

[8] I. De Marco, E. Reverchon, Influence of pressure, temperature and concentration on the mechanisms of particle precipitation in supercritical antisolvent micronization, J. Supercrit. Fluids 58 (2011) 295-302.

[9] E. Reverchon, Supercritical-assisted atomization to produce micro- and/or nanoparticles of controlled size and distribution, Ind. Eng. Chem. Res. 41 (2002) 2405-2411.

[10] M. Türk, P. Hils, B. Helfgen, K. Schaber, H.-J. Martin, M.A. Wahl, Micronization of pharmaceutical substances by the Rapid Expansion of Supercritical Solutions (RESS): a promising

method to improve bioavailability of poorly soluble pharmaceutical agents, J. Supercrit. Fluids 22 (2002) 75-84.

[11] D. Bolten, M. Türk, Micronisation of carbamazepine through rapid expansion of supercritical solution (RESS), J. Supercrit. Fluids 62 (2012) 32-40.

[12] N. Falco, E. Reverchon, G. Della Porta, Injectable PLGA/hydrocortisone formulation produced by continuous supercritical emulsion extraction, Int. J. Pharm. 441 (2013) 589-597.

[13] D. Li, Y. Xia, Electrospinning of Nanofibers: Reinventing the Wheel?, Adv. Mater. 16 (2004) 1151-1170.

[14] N. Bhardwaj, S.C. Kundu, Electrospinning: A fascinating fiber fabrication technique, Biotechnol. Adv. 28 (2010) 325-347.

[15] Z.-M. Huang, Y.-Z. Zhang, M. Kotaki, S. Ramakrishna, A review on polymer nanofibers by electrospinning and their applications in nanocomposites, Compos. Sci. Technol. 63 (2003) 2223-2253.

[16] A. Jaworek, Micro- and nanoparticle production by electrospraying, Powder Technol. 176 (2007) 18-35.

[17] J.A. Bhushani, C. Anandharamakrishnan, Electrospinning and electrospraying techniques: potential food based applications, Trends Food Sci. Technol. 38 (2014) 21-33.

[18] P. Mehta, R. Haj-Ahmad, M. Rasekh, M.S. Arshad, A. Smith, S.M. van der Merwe, X. Li, M.-W. Chang, Z. Ahmad, Pharmaceutical and biomaterial engineering via electrohydrodynamic atomization technologies, Drug Discovery Today 22 (2017) 157-165.

[19] P. Gupta, C. Elkins, T.E. Long, G.L. Wilkes, Electrospinning of linear homopolymers of poly(methyl methacrylate): exploring relationships between fiber formation, viscosity, molecular weight and concentration in a good solvent, Polymer 46 (2005) 4799-4810.

[20] V. Beachley, X. Wen, Effect of electrospinning parameters on the nanofiber diameter and length, Mater. Sci. Eng. C 29 (2009) 663-668.

[21] N. Levit, G. Tepper, Supercritical CO_2-assisted electrospinning, J. Supercrit. Fluids 31 (2004) 329-333.

[22] B. Lee, D. Freitag, W. Arlt, M. McHugh, Hollow fibers by electrospinning in supercritical CO_2, Mater. Sci. 2 (2007).

[23] J. Liu, Z. Shen, S.-H. Lee, M. Marquez, M.A. McHugh, Electrospinning in compressed carbon dioxide: Hollow or open-cell fiber formation with a single nozzle configuration, J. Supercrit. Fluids 53 (2010) 142-150.

[24] L. Li, Z. Jiang, Q. Pan, T. Fang, Producing Polymer Fibers by Electrospinning in Supercritical Fluids, J. Chem. 2013 (2013).

[25] K. Okamoto, Wahyudiono, Fabrication of micro-hollow fiber by electrospinning process in near-critical carbon dioxide, AIP Conference Proceedings 43 (2014) 1586.

[26] Wahyudiono, S. Machmudah, H. Kanda, S. Okubayashi, M. Goto, Formation of PVP hollow fibers by electrospinning in one-stepprocess at sub and supercritical CO_2, Chem. Eng. Process. 77 (2014) 1-6.

[27] L. Li, J. Xu, T. Fang, J. Geng, D. Freitag, W. Arlt, Producing PVP nanofibers by electrospinning in N_2, Adv. Mater. Res. 560-561 (2012) 701-708.

[28] N. Falco, E. Kiran, Volumetric properties of ethyl acetate + carbon dioxide binary fluid mixtures at high pressures, J. Supercrit. Fluids 61 (2012) 9-24.

[29] E Kiran, P.G. Debenedetti, C.J. Peters, Supercritical fluids: fundamentals and applications, 2012.

[30] L.P. Cunico, C. Turner, Supercritical fluids and gas-expanded liquids, The Application of Green Solvents in Separation Processes, chapter 7 (2017) 155-177.

[31] L. Baldino, S. Cardea, E. Reverchon, Supercritical Assisted Electrospray: An Improved Micronization Process, Polymers 11 (2019) 244-255.

[32] S.N. Joung, C.W. Yoo, H.Y. Shin, S.Y. Kim, K.-P. Yoo, C.S. Lee, W.S. Huh, Measurements and correlation of high-pressure VLE of binary CO_2–alcohol systems (methanol, ethanol, 2-methoxyethanol and 2-ethoxyethanol), Fluid Phase Equilib. 185 (2001) 219-230.

[33] H. Tanaka, M. Kato, Vapor-liquid equilibrium properties of carbon dioxide + ethanol mixture at high pressures, J. Chem. Eng. Jpn. 28 (1995) 263-266.

[34] E.M. Abdelrazek, I.S. Elashmawi, S. Labee, Chitosan filler effects on the experimental characterization, spectroscopic investigation and thermal studies of PVA/PVP blend films, Phys. B 405 (2010) 2021-2027.